

Laboratory Studies of Butane Nucleation on Organic Haze Particles: Application to Titan's Clouds

Daniel B. Curtis,^{†,‡} David L. Glandorf,^{†,‡} Owen B. Toon,^{§,⊥} Margaret A. Tolbert,^{*,†,‡} Christopher P. McKay,^{||} and Bishun N. Khare^{||}

Department of Chemistry and Biochemistry, Cooperative Institute for Research in Environmental Sciences, Department of Astrophysical and Planetary Sciences, and Laboratory for Astrophysical and Space Physics, University of Colorado, Boulder, Colorado 80309, and Space Science Division, NASA Ames Research Center, Moffett Field, California 94035

Received: September 28, 2004; In Final Form: December 3, 2004

Titan, Saturn's largest satellite, has a thick nitrogen/methane atmosphere with various hydrocarbons present in minor amounts. Recent observations suggest that CH₄ may condense to form clouds near the moon's tropopause. Titan's methane cloud formation is probably triggered by a sequential nucleation of hydrocarbons onto Titan's haze material as tropospheric convection occurs due to differential heating of the surface or as the haze settles through the lower stratosphere. To better constrain Titan's cloud formation mechanism, investigations of the nucleation of several hydrocarbons will be necessary. Butane was chosen for this study because it has a relatively high freezing point and is estimated to be present at 200 part per billion levels. If this amount of butane were to condense on each haze particle, a visible cloud would be observed. Laboratory measurements at $T = 125$ K were performed to determine the relative ease of solid butane nucleation onto laboratory-produced tholin particles having an elemental composition of C₅H₅N, and solid films of hexane and acetonitrile. We find that butane nucleation onto the haze particles requires a relatively high saturation ratio of $S > 1.30$. Because butane nucleation is difficult, it may occur on only a very small subset of the total haze particles available. Such selective nucleation of butane would lead to those particles becoming coated with significant amounts of butane. Requiring a high saturation ratio for butane nucleation will reduce the optical depth of butane clouds by a factor of 100 because the particles will be fewer in number for a given condensed mass.

I. Introduction

Titan, Saturn's largest satellite, is unusual because it is the only moon in our solar system that is known to have a substantial atmosphere. This atmosphere consists of approximately 95% nitrogen, N₂, and a few percent methane, CH₄.^{1,2} Minor constituents include argon, which may be present in amounts up to a few percent, and larger hydrocarbon species, the most abundant of which is ethane, C₂H₆, present at a mixing ratio of about 20 parts per million by volume (ppmv).² Titan's thick atmosphere results in a surface pressure of 1.5 atm, 50% higher than that of Earth. Titan's temperature is much colder than Earth's, falling from 95 K at the surface to 75 K at the tropopause, and then rising to 180 K in the stratosphere.³

An intriguing feature of Titan's atmosphere is the presence of a thick reddish-brown haze that completely shrouds the surface. These haze particles, produced photochemically in Titan's upper atmosphere approximately 300 km above the surface, are thought to be composed of solid organic species.⁴ They are expected to fall through the atmosphere and are thought

to have accumulated on Titan's surface over time. Solid materials have been produced from laboratory simulations of various atmospheres for many years.^{5,6} They were dubbed "tholins" by Sagan and Khare,⁷ a general term that applies to any solid material produced by the laboratory reaction of a mixture of various cosmically abundant gases. Tholins produced in a laboratory experiment specifically designed to simulate Titan are sometimes termed "Titan tholins". Khare et al.⁴ showed that this laboratory-produced solid material (using a gas mixture of 90% N₂ and 10% CH₄) is a relatively good optical match for the haze present in Titan's atmosphere.

Another unusual feature of Titan's atmosphere is that the low temperature, coupled with the abundant hydrocarbons present, leads to an atmosphere in which the hydrocarbons may condense. If true, clouds of condensed hydrocarbons, such as ethane and methane, could be present in Titan's troposphere or lower stratosphere.⁸ Ethane, and possibly methane, should also be saturated near Titan's surface, implying that they could be present in a condensed state on the surface, perhaps in a liquid state.^{9,10} This evokes a situation on Titan which is analogous to Earth's hydrologic cycle, with the exception that the clouds, rain, and reservoirs on the surface of Titan would consist of liquid hydrocarbons rather than liquid water. If these liquid reservoirs are present, Titan would be the only planet or moon in our solar system, other than Earth, to have liquid on its surface.

Past analyses of observational data from the Voyager spacecraft suggest that methane is supersaturated in Titan's

* Corresponding author. Phone: (303) 492-3179. Fax: (303) 492-1149. E-mail: tolbert@colorado.edu.

[†] Department of Chemistry and Biochemistry, University of Colorado.

[‡] Cooperative Institute for Research in Environmental Sciences, University of Colorado.

[§] Department of Astrophysical and Planetary Sciences, University of Colorado.

[⊥] Laboratory for Astrophysical and Space Physics, University of Colorado.

^{||} Space Science Division, NASA Ames Research Center.

lower atmosphere.^{11–13} In addition, McKay¹⁴ reported a very low solubility for laboratory-produced Titan haze material in liquid propane, suggesting that hydrocarbon nucleation onto Titan's haze particles may be difficult, consistent with methane supersaturation.¹¹ However, recent Earth-based observations of short-lived clouds in Titan's atmosphere have also been reported,^{15,16} implying that cloud formation may be a common, even daily, occurrence. The observations reported by Brown et al.¹⁷ and Roe et al.¹⁸ confirmed the presence of clouds near Titan's south pole. Supersaturation and cloud formation are not necessarily mutually exclusive; it is possible to have a supersaturation of methane and cloud formation if there are too few cloud condensation nuclei for cloud condensation to pull down the supersaturation as the clouds grow. Supersaturation can also occur if nucleation onto the particles is difficult so that cloud particles do not form readily.

The cloud condensation nuclei likely to be present at Titan's tropopause are haze particles formed in the upper atmosphere that have slowly fallen or diffused toward the surface. As the particles diffuse or as convective lifting occurs, they will encounter areas where hydrocarbon gases are saturated and might condense. If these higher hydrocarbons condense readily, one would expect all of the available tholin particles to be very similar chemically, with a coating of hydrocarbons. In contrast, if hydrocarbon nucleation on the haze particles is difficult, a few particles will become more fully coated while the rest remain bare. The condensation nuclei at the tropopause in this scenario would be more diverse, setting up a situation where methane might preferentially condense on only a subset of the total condensation nuclei present. In addition, relatively difficult nucleation onto the haze particles will reduce the optical depth of any clouds formed because the particles will be fewer in number.

Hydrocarbon nucleation in the outer solar system was studied extensively by the nucleation models of Moses et al.,¹⁹ yet no laboratory data exist to our knowledge. In the current work, we examine the nucleation of a higher order hydrocarbon, butane, onto tholin particles and several other hydrocarbon films. We chose butane because it has a relatively high freezing temperature and was therefore convenient for our initial laboratory studies, and to validate the experimental procedure. Although butane has not yet been detected in Titan's atmosphere, its abundance can be estimated by comparing the butane and propane productions from the photochemical model of Lara et al.²⁰ A simple scaling to the propane concentration yields an estimation of the butane concentration of ~200 parts per billion by volume (ppbv). In addition, a recent laboratory measurement showed a high production of butane gas from the ultraviolet irradiation of pure methane, comparable to the production rate of ethane,²¹ so butane should be present in significant amounts in Titan's atmosphere. The butane will be highly supersaturated in Titan's lower stratosphere and should be present on the haze particles as they settle toward Titan's surface. This amount of butane will fully coat all of the haze particles present if nucleation occurs onto each haze particle. We measure the critical saturation ratio, S_{crit} , required for butane nucleation on laboratory-produced particles and films, defined as

$$S_{\text{crit}} = P_{\text{nuc}}/P_{\text{vap}}(T) \quad (1)$$

where P_{nuc} is the butane pressure at nucleation and $P_{\text{vap}}(T)$ is the saturation vapor pressure of butane at the same temperature. We then use heterogeneous nucleation theory to predict the saturation ratio expected for butane nucleation on very small

Titan haze particles. Finally, we discuss the implications of this work for Titan cloud formation.

II. Experimental Section

A. Haze Analogue Production. Several different energy sources have been employed for the laboratory production of solar system haze analogues, including irradiation by ultraviolet light^{22,23} and application of a high-frequency discharge to the outside of a glass reaction vessel.²⁴ Another common technique is the application of a direct current (dc) or alternating current (ac) electrical spark to the mixture across an electrode gap inside the vessel.^{14,25}

We have used the latter technique with a cylindrical glass reaction vessel containing two tungsten electrodes piercing the glass walls and meeting at the center of the vessel, with a gap between them of ~1 cm. The vessel is 25 cm in length and 6 cm in inside diameter (~700 cm³ in volume) and is equipped with a Viton O-ring which allows the vessel to be opened and objects placed inside. For this study a silicon wafer with a diameter of 2.5 cm was placed in the bottom of the vessel for deposition of the tholin particles. The reaction vessel was evacuated to a pressure of ~20 mTorr using a mechanical pump and then filled with a gas mixture composed of 90.00% N₂ and 10.00% CH₄ (research grade, Airgas Intermountain) until a pressure of 300 ± 50 Torr was reached, as monitored by a Convectron Pirani thermal conduction pressure gauge (Granville-Phillips). The vessel was then isolated from the pump, and the gas mixture was exposed to a spark discharge from a hand-held high-frequency generator, or Tesla coil (Fisher Scientific). The spark discharge is an ac current with a frequency of 60 Hz and a voltage across the gap of approximately 10 000 V. The silicon wafer rested directly underneath the gap between the electrodes, which facilitated an evenly distributed deposition of the particles onto the silicon wafer. The gas mixture was flushed out and replaced each hour. After 12 h, the wafer was flipped to expose its other side. This process was repeated until each side of the wafer had been exposed for 24 h, a total exposure time of 48 h. The particles appear as a film of a brown solid material and coat the wafer, as well as the inside walls of the glass vessel. Scanning electron microscope (SEM) images of the particles generated using this procedure by deposition on aluminum foil (a simpler substrate for SEM than the silicon wafers used in the nucleation experiments) for 12 h are shown in Figure 1. The images show complete coverage of particles with little exposed aluminum foil. Thus, it can be assumed that after 24 h of exposure per side there is essentially no bare silicon remaining on the wafers used in the nucleation experiments. Figure 1B shows the particles under greater magnification. The particle film appears to be an aggregate of 0.5 μm diameter particles.

Figure 2 shows an FTIR spectrum of the tholin particles after deposition onto a silicon wafer, taken using a Nicolet Magna 550 Fourier transform infrared spectrometer. The spectral region shown (3650–1750 cm⁻¹) was chosen to ensure a qualitative incorporation of nitrogen atoms into the haze. The spectrum shown is the ratio of observed absorbance to the spectrum's background (the same Si wafer prior to deposition of the particles) and shows only the tholin material. The area centered at 2350 cm⁻¹ had two large negative peaks which were removed for clarity. These peaks are due to CO₂ gas and were present in the spectrum due to slight changes in the gases present outside of the chamber since the spectra were taken weeks apart in time. The key features in the spectrum are a peak at 2200 cm⁻¹, indicative of the –CN triple bond stretch,⁴ and a broad –N–H

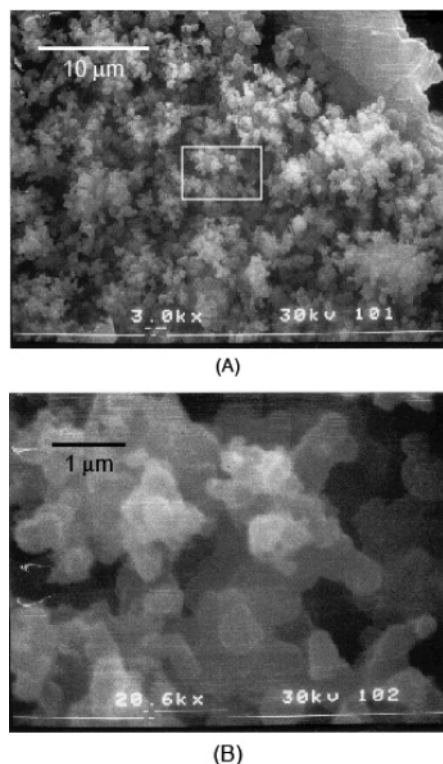


Figure 1. Scanning electron microscopy images of laboratory-produced Titan tholin particles under (A) low and (B) high magnification. Image B corresponds to the rectangular area highlighted in image A. The exposed area in the upper right corner of image A is an artifact of cutting the aluminum foil in preparation for transfer to the electron microscope.

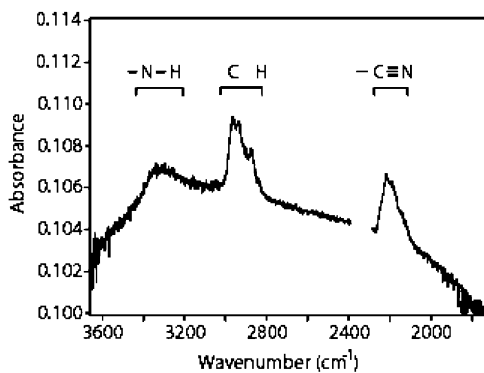


Figure 2. FTIR spectrum of laboratory-produced tholin particles. The gap at 2390–2285 cm^{-1} is due to the gas-phase CO_2 peaks at 2362 and 2338 cm^{-1} , which were removed from the spectrum for clarity.

stretch at 3200–3400 cm^{-1} . These features indicate that nitrogen atoms are being incorporated into the solid haze material.²⁶

In addition to the FTIR spectrum of the haze analogue material, nitrogen incorporation was confirmed through elemental analysis. After several weeks of exposure to the spark discharge, enough material (~ 12 mg) was scraped off the inside walls of the vessel to perform elemental analysis for C, H, N, and O. The analysis was performed at Desert Analytics (Tucson, AZ) in triplicate on one sample. The particles were found to contain $62.69 \pm 0.85\%$ C, $5.06 \pm 0.08\%$ H, $14.11 \pm 0.34\%$ N, and $16.40 \pm 0.35\%$ O by mass. The oxygen atoms in the sample are likely present from oxidation by O_2 when the sample was exposed to air¹⁴ for several weeks prior to the elemental analysis, but could be from residual H_2O vapor in the reaction vessel after pumping down. Water in the vessel could be present at levels possibly up to a few hundred parts per million by volume.

TABLE 1: Elemental Analysis Comparison

reference	stoichiometry	C/N ratio	conditions
Sagan et al. (1984) ²⁹	$\text{C}_8\text{H}_{13}\text{N}_4$	1.9	$P > 7$ Torr
Coll et al. (1995) ³¹	$\text{C}_{11}\text{H}_{11}\text{N}$	11	$T \approx 100$ K
McKay (1996) ¹⁴	$\text{C}_{11}\text{H}_{11}\text{N}_2$	5.5	$T \approx 298$ K, $P \approx 850$ Torr
Coll et al. (1999) ³²	$\text{C}_{11}\text{H}_4\text{N}_{14}$	2.8	$T \approx 100$ – 150 K, $P \approx 1.5$ Torr
this study	$\text{C}_5\text{H}_5\text{N}$	5.17	$T \approx 298$ K, $P \approx 300$ Torr

There is relatively little O_2 (~ 10 ppmv) and H_2O (~ 3 ppmv) in the gas mixture itself. The elemental analysis excluding oxygen results in an empirical formula of $\text{C}_5\text{H}_5\text{N}$, with a true C/N ratio of 5.17. McKay et al.²⁷ and Lebonnios et al.²⁸ reviewed empirical formulas from previous studies, which are shown for comparison in Table 1. Sagan et al.²⁹ and McKay¹⁴ showed oxygen in the sample at a weight percent of 17% and 11.0%, respectively, similar to this study. The result for the elemental composition of our material most closely resembles that of McKay¹⁴ in both elemental stoichiometry and experimental conditions.

It is possible that the O atoms present in the solid affect its properties as a substrate for nucleation. However, the samples used in the experiments were exposed to air for ~ 20 min while being transferred into the high-vacuum chamber, so they probably had less oxygen present (but possibly percent levels) than the samples sent for elemental analysis, which were exposed to air for several weeks. For example, using a system optimized to reduce oxygen contamination, Tran et al.³⁰ found that oxidation of their simulated Titan haze rose from a value of 1.4% O to 7.2% O upon exposure to air for 7 days. The solid material produced in the Coll et al.^{31,32} studies was transferred under nitrogen, eliminating the possibility of atmospheric contamination of the sample.

B. Nucleation Experiments. Nucleation experiments were performed in a stainless steel vacuum chamber, shown schematically in Figure 3. The chamber is equipped with a leak valve for the introduction of butane gas, an MKS Baratron capacitance manometer gauge to monitor the pressure of the introduced gas, and an FTIR spectroscopic probe of the condensed phase. The temperature of the silicon wafer was controlled through a combination of liquid-nitrogen cooling and resistive heating and is monitored by a type T thermocouple. Experiments were performed on the blank silicon wafer, the silicon wafer coated with tholin particles, or the silicon wafer coated with organic films.

In a typical experiment, the chamber was first evacuated and the temperature lowered to ~ 125 K. The nucleation point was

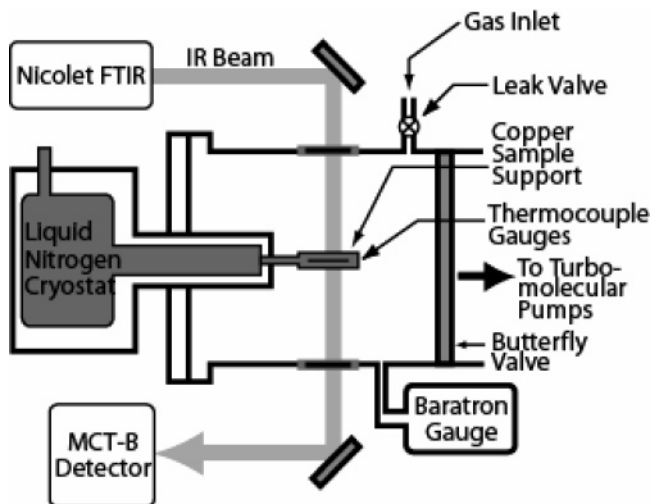


Figure 3. Schematic diagram of the experimental apparatus.

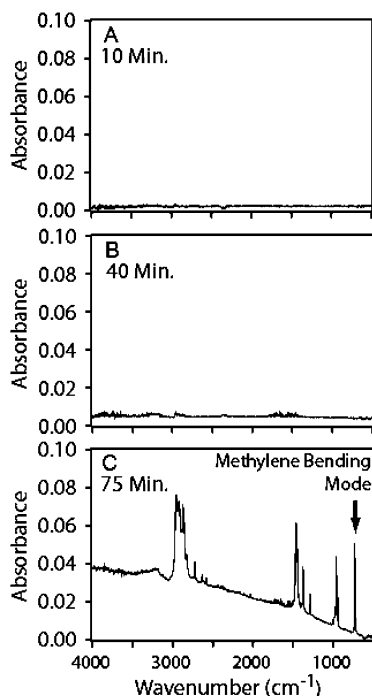


Figure 4. Infrared spectra obtained during a butane nucleation experiment on Titan tholin particles.

determined by slow increases in the butane pressure in the chamber. The pressure was allowed to equilibrate for >30 s if no nucleation occurred immediately upon the increase. After 30 s, the pressure was increased slightly (approximately 0.01–0.02 mTorr) and the process repeated until nucleation occurred. The nucleation pressure was typically 0.5–2.5 mTorr, depending on the temperature and the supersaturation required. When nucleation occurred, it was detected very rapidly (within 4 s, the time resolution of the FTIR), marked by a sharp increase in the FTIR spectrum and a sharp drop in the pressure in the chamber.

III. Results

For studies of nucleation on tholin particles, we first coated a silicon wafer with tholin particles and then transferred it under air into a copper mount inside the stainless steel vacuum chamber described above. The chamber was then pumped out to a pressure of $\sim 1 \times 10^{-7}$ Torr, and the tholin-coated silicon wafer was cooled and maintained at a temperature of ~ 125 K. The experiments were then begun by introducing butane vapor into the chamber.

A typical experiment on tholin particles is shown in Figures 4 and 5. Selected FTIR spectra for the experiment are shown in Figure 4, along with the corresponding time that they were taken. From the start of the experiment, the absorbance was measured as the ratio to the spectrum of the initial tholin material for clarity. Therefore, the spectrum of the tholin material is not observed. At $t = 10$ min, butane vapor had been added to the chamber, but at a pressure below that expected for nucleation to occur. No butane was present in the condensed phase, as shown by the FTIR spectrum taken at that time. The pressure of butane is too low (0.5–5.0 mTorr) in all experiments to see gas-phase butane features in the spectrum. Figure 5 shows the butane saturation ratio (left axis) converted from butane pressure and the integrated absorbance of the butane peak at 745–725 cm^{-1} (right axis) versus time during the experiment. This IR peak is the in-phase methylene rock (bending mode) at 731 cm^{-1}

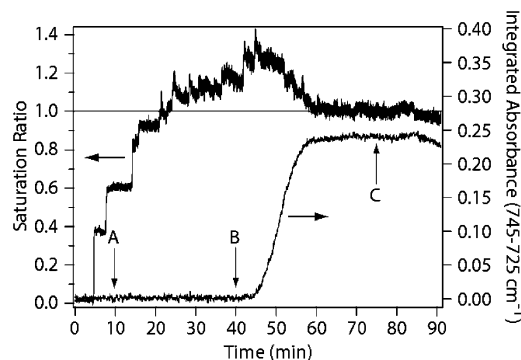


Figure 5. Saturation ratio and integrated absorbance during butane nucleation on Titan tholin particles. The arrows at A, B, and C correspond to the spectra shown in Figure 4A–C, respectively. The top trace shows saturation ratio as a function of time plotted on the left axis. The bottom trace shows integrated absorbance of one butane peak as a function of time plotted on the right axis.

and was chosen due to its sharpness and the fact that it appears only in the solid phase of butane.³³ The pressure of butane was then incrementally increased until the butane vapor was supersaturated. At $t = 40$ min, the butane saturation ratio was greater than 1.0, yet nucleation had not occurred, as confirmed by the FTIR spectrum shown in Figure 4B. The pressure was further increased until nucleation occurred at $t = 45$ min, as determined by the rise of the integrated absorbance of the butane peak at 745–725 cm^{-1} . The full spectrum in Figure 4C at $t = 75$ min shows the sharp methylene bending mode in solid butane. In addition, the nucleation point is confirmed by a drop in butane pressure in the chamber such that the saturation ratio approached unity after nucleation began.

A slight decay in the butane signal was often observed prior to nucleation. A similar decay was observed in experiments performed at room temperature, and thus we believe the gas in the feed line was slowly being depleted during the experiment. However, we cannot rule out a slight condensation of butane on a cold spot in the chamber not probed by the infrared beam. This should not, however, impact our results, as experiments show that our entire silicon wafer was at a uniform temperature and thus the entire surface was exposed to butane at a single saturation ratio.

After the butane had condensed onto the haze material, a frost point calibration was performed. To do this, the pressure was adjusted to a point where the film neither grew nor desorbed, as determined by the integrated absorbance of the butane peak at 745–725 cm^{-1} . This pressure is defined to be the solid butane vapor pressure. For this study, the vapor pressure of solid butane was measured to be in the range of 0.5–5 mTorr at temperatures ranging from 120 to 126 K. This range of vapor pressures is consistent with those measured for liquid butane at higher temperatures and extrapolated to temperatures of the solid phase.¹⁹ While the solid vapor pressure likely differs from the liquid vapor pressure, we were not able to find values for the solid vapor pressure. These values were used simply to confirm a general consistency and were not needed to calculate the saturation ratio. The critical saturation ratio (that saturation ratio required to obtain nucleation), S_{crit} , was determined via $S_{\text{crit}} = P_{\text{nucl}}/P_{\text{vap}}$, where P_{nucl} is the measured pressure in the chamber when nucleation occurs and P_{vap} is the butane vapor pressure determined in the frost point calibration. Because both the nucleation pressure and the vapor pressure are determined in one experiment, we have an internal calibration which yields high accuracy in the saturation ratio determined.

The experiment shown in Figures 4 and 5 yields $S_{\text{crit}} = 1.35$. A total of five experiments were performed on tholin particles with an average value of $S_{\text{crit}} = 1.30 \pm 0.06$ over a temperature range of 121.9–124.0 K. Over this temperature range, no temperature dependence was observed in S_{crit} . The range of values reported is the average value for the five experiments plus or minus the standard deviation of the five experiments.

Further experiments were performed on a blank silicon wafer to ensure that nucleation was not occurring on any exposed silicon that remained even after the wafer was coated with tholin material. Butane nucleation onto bare silicon was performed in seven experiments over a temperature range of 121.6–125.0 K with an average value of $S_{\text{crit}} = 1.47 \pm 0.22$. Thus, even if bare silicon is present during the experiments, butane nucleation onto the silicon is relatively difficult. Therefore, butane will more readily nucleate on the tholin particles than onto any bare silicon that may be present.

Butane nucleation was also studied on films of water ice. Although water is not likely to exist in appreciable amounts in Titan's atmosphere, it may be present in trace amounts during meteor or comet ablation in Titan's upper atmosphere. However, it is mainly of interest in this study due to the fact that background water in the chamber could condense onto the silicon wafer or haze analogue material as it is cooled prior to a nucleation experiment. Butane nucleation onto water ice was performed in 11 experiments over a temperature range of 122.8–125.0 K with an average value of $S_{\text{crit}} = 1.59 \pm 0.12$. This is higher than the S_{crit} we measure on the tholin particles. Therefore, we are confident that we are measuring butane nucleation on the organic material itself, rather than on water ice that might have condensed during cooling.

We have also performed additional experiments of butane nucleation onto films of *n*-hexane (C_6H_{14}) and acetonitrile (CH_3CN) to determine if we can find any surface that facilitates nucleation. Hexane (and other higher molecular weight hydrocarbons) and acetonitrile (and various nitriles, particularly HCN) may be present in Titan's atmosphere due to the photochemical processing of methane. If hexane and acetonitrile are present in Titan's atmosphere, they will almost certainly be present in the condensed phase (most likely on the haze particles) in the stratosphere due to their low vapor pressures at those temperatures.

In these experiments, a blank silicon wafer was placed inside the vacuum chamber and the chamber evacuated to a pressure of $\sim 1 \times 10^{-7}$ Torr. The wafer was then cooled and maintained at ~ 125 K. A film of hexane or acetonitrile was then grown onto the blank silicon wafer. These films were grown with a backfill valve, thus coating both sides of the wafer and leaving no bare silicon exposed to act as a possible nucleation site.

After the organic film was grown, the chamber was evacuated and the pressure reduced to the 10^{-7} Torr level. Because the vapor pressures of hexane and acetonitrile at these temperatures are so low, no change was seen in the film spectrum after > 30 min. Most films were allowed to equilibrate for much shorter time periods, on the order of 5–10 min. After evacuation of the gas-phase hexane or acetonitrile, butane was introduced into the chamber at a pressure below that expected for nucleation to occur, as in the tholin experiments.

A typical film experiment for butane nucleation onto acetonitrile is shown in Figures 6 and 7. At $t = 1$ min, the wafer had been cooled, but no vapor had been added to the chamber and no signal was observed in the FTIR spectrum shown in Figure 6A. From $t = 3$ –10 min, the solid acetonitrile film was grown. At $t = 12$ min, the pressure in the chamber had dropped down

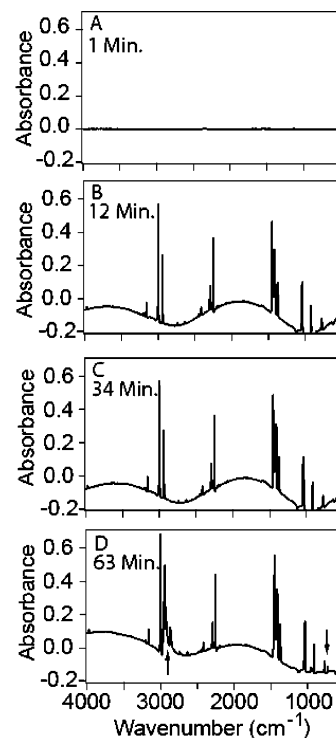


Figure 6. Infrared spectra obtained during butane nucleation on a solid acetonitrile film.

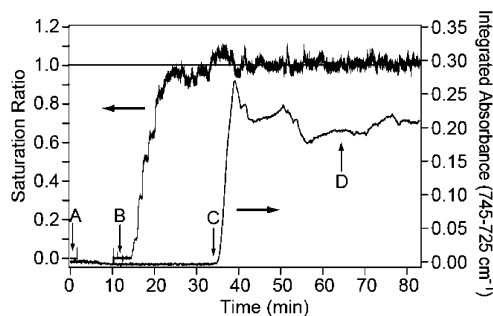


Figure 7. Saturation ratio and integrated absorbance during butane nucleation on a solid acetonitrile film. The top trace shows saturation ratio as a function of time plotted on the left axis. The bottom trace shows the integrated absorbance of a butane peak as a function of time plotted on the right axis. The arrows at A, B, C, and D correspond to the spectra shown in Figure 6A–D, respectively.

to the background pressure and the film was stable. The FTIR spectrum taken at that time (Figure 6B) shows the acetonitrile film on the silicon wafer. The films typically produced an interference pattern in the FTIR spectrum, indicating that they are relatively thick and flat.³⁴ This interference pattern occurs in the FTIR spectrum when light reflecting off of the growing film interferes with light reflected from the film/Si interface. Constructive interference occurs when the path difference is an integral number of wavelengths. Since this interference depends on wavelength, a wavelike pattern is observed in the FTIR spectra after the substrate film is deposited and can be used to determine film thickness. The acetonitrile films were calculated to vary from 0.49 to 6.89 $\mu\text{m per side}$ (total thickness is twice this value).

Figure 6C, taken at $t = 34$ min, shows that no butane nucleation has occurred onto the acetonitrile film, despite the supersaturated condition for butane in the chamber (seen in Figure 7 at $t = 34$ min). Figure 6D shows the FTIR spectrum at $t = 63$ min after butane nucleation has occurred. Characteristic butane peaks can be seen around 2800 (C–H stretches) and

TABLE 2: Summary of Results

substrate	$S_{\text{crit}} \pm \sigma$	contact parameter, $m \pm \sigma$
Titan tholin particles	1.30 ± 0.06	0.966 ± 0.007
hexane	1.36 ± 0.11	0.960 ± 0.011
acetonitrile	1.13 ± 0.06	0.983 ± 0.007
water ice	1.59 ± 0.12	0.938 ± 0.010
bare silicon	1.47 ± 0.22	0.951 ± 0.019

731 cm^{-1} (the methylene rock (bending mode)), as highlighted with arrows. Butane nucleation onto solid acetonitrile was performed in eight experiments over a temperature range of 120.5–126.2 K, with an average value of $S_{\text{crit}} = 1.13 \pm 0.06$. No temperature dependence was observed in S_{crit} over the temperature range of this study. However, we did note a small dependence of S_{crit} on the acetonitrile film thickness. For acetonitrile, S_{crit} decreased with thickness linearly from a value of $S_{\text{crit}} = 1.15$ at a thickness of $0.49 \mu\text{m}$ to a value of $S_{\text{crit}} = 1.07$ at a thickness of $4.07 \mu\text{m}$. However, S_{crit} did not seem to vary above a thickness of $4.07 \mu\text{m}$ up to the highest thickness of $6.89 \mu\text{m}$. It is unclear why S_{crit} varies with substrate film thickness. The thinner and thicker films are both flat (as confirmed by the interference pattern present in each), but it may be that the thicker films are slightly less uniform, thus providing imperfections in the surface which encourage nucleation. We find that butane nucleation on hexane requires a critical saturation ratio of $S_{\text{crit}} = 1.36 \pm 0.11$ with no temperature dependence over the range of this study. Further, there was no detectable variation in S_{crit} with hexane film thickness from 0.32 to $3.3 \mu\text{m}$ per side.

A comparison of all the values of S_{crit} determined in this work, along with the corresponding standard deviations, is given in Table 2. In addition to the values of S_{crit} , we have also included the values for the contact parameter, m , in Table 2. These values were calculated using a classical nucleation theory method described in the Appendix. The contact parameter can be used to predict how readily butane nucleation occurs on the very small particles expected in Titan's atmosphere.

IV. Application To Titan's Clouds

Butane is only one of a number of hydrocarbons and nitriles that will condense on the haze particles in Titan's atmosphere. It is possible that butane nucleation also occurs onto other organic solids such as HCN, acetylene, or pentane. To fully understand the formation of Titan's clouds, experiments may be needed for several of these species. This study has probed the possibility that some of the Titan haze particles may be coated with a layer of butane at the tropopause. If this is the case, butane condensation may impact Titan's cloud formation mechanism.

We find that butane requires a saturation ratio of $S > 1.30$ in order to nucleate onto laboratory-produced tholin material of $0.25 \mu\text{m}$ radius. Previous work suggests that Titan's haze particles are smaller than those we have produced for this study, with a radius of $0.1\text{--}0.2 \mu\text{m}$,³⁵ or are aggregates of small curved particles.²⁷ As shown in the Appendix using nucleation theory, if butane nucleates on a flat surface with $S_{\text{crit}} = 1.3$, the value increases to $S_{\text{crit}} = 1.5$ for particles of radius $r_N = 0.1 \mu\text{m}$, and increases to $S_{\text{crit}} \approx 1.8$ if Titan's haze particles are smaller, with $r_N = 0.05 \mu\text{m}$. Thus, nucleation theory supports an even higher degree of supersaturation if the particles in Titan's haze are smaller than $0.1 \mu\text{m}$, or are aggregates of small particles with a high degree of curvature.

Although butane has not been detected directly, photochemical modeling²⁰ predicts that it is present in significant amounts

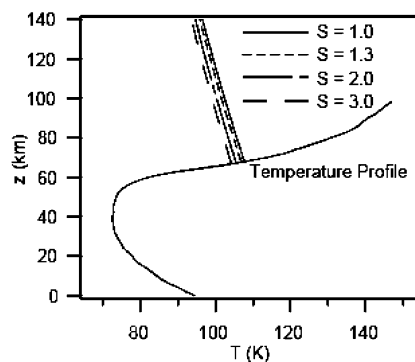


Figure 8. Vapor saturation profiles vs altitude and temperature profile. The saturation profiles are the temperatures at which the actual butane pressure corresponds to a saturation ratio of $S = 1.0, 1.3, 2.0,$ and $3.0,$ respectively. Therefore, nucleation will occur for each scenario at the altitude at which the vapor saturation profile temperature equals the actual temperature in Titan's atmosphere.

in Titan's atmosphere (~ 200 ppbv), and a recent laboratory study shows a high production rate of butane when methane is irradiated with UV light.²¹ Given an abundance of 200 ppbv, we can calculate the temperature and hence altitude at which butane nucleation will occur. Figure 8 shows the saturation temperature and Titan's temperature profile plotted as a function of altitude. Nucleation should occur for each scenario when the vapor saturation line crosses the temperature profile. Using this calculation, we predict that butane nucleation will occur at an altitude of ~ 68 km and a temperature of ~ 108 K if a saturation ratio of $S = 1.0$ is required. If a saturation ratio of $S = 1.3$ is required, there is a small shift in the temperature and altitude at which nucleation will occur to an altitude of 67 km and a temperature of 107 K. While the condensation altitude of butane does not change dramatically with S_{crit} , we find that the distribution of butane on the haze particles will vary greatly with the value of S_{crit} assumed.

We can estimate the amount of butane which will coat the haze particles in Titan's atmosphere by using a steady-state approximation in a simple one-dimensional model of a horizontal slice of Titan's atmosphere, equating the photochemical production rate of butane by mass (P , the flux into the layer) and the mass loss rate due to condensation of the butane (L , the flux out of the layer to particles that can fall out of the layer).

$$P (\text{g cm}^{-2} \text{ s}^{-1}) = L (\text{g cm}^{-2} \text{ s}^{-1}) \quad (2)$$

Here, $P = 6.55 \times 10^6 \text{ molecules cm}^{-2} \text{ s}^{-1}$ ($6.31 \times 10^{-16} \text{ g cm}^{-2} \text{ s}^{-1}$),²⁰ and L is the product of the mass concentration of particles, $M_{\text{particles}} (\text{g cm}^{-3})$, and the fall velocity of the particles, $V_{\text{fall}} (\text{cm s}^{-1})$,

$$L = M_{\text{particles}} V_{\text{fall}} \quad (3)$$

$M_{\text{particles}}$ can be determined via

$$M_{\text{particles}} = n_{\text{particles}} \rho_{\text{particles}} (4/3)\pi r^3 \quad (4)$$

where $n_{\text{particles}}$ is the number of particles per cubic centimeter, $\rho_{\text{particles}}$ is the density of butane, 0.760 g cm^{-3} (at $T = 108 \text{ K}$), and r is the particle radius.

V_{fall} is dependent on radius as

$$V_{\text{fall}} = V_0 r \quad (5)$$

where $V_0 = 50 \text{ s}^{-1}$ at 70 km in Titan's atmosphere.³⁶ Therefore, substituting eqs 3, 4, and 5 into eq 2 gives

$$P = n_{\text{particles}} \rho_{\text{particles}} (4/3) \pi r^3 V_0 r \quad (6)$$

Solving for r allows us to calculate the radius of condensed butane particles via

$$r = [P / (n_{\text{particles}} \rho_{\text{particles}} (4/3) \pi V_0)]^{1/4} \quad (7)$$

If nucleation occurs onto every particle, $n_{\text{particles}}$ equals the number of haze particles present at 68 km, 150 cm^{-3} .³⁶ Using this approach, if butane nucleation occurs readily onto each particle ($S_{\text{crit}} = 1$), the particles would reach a total radius of $0.13 \text{ }\mu\text{m}$ of solid butane (ignoring the haze particle itself), which will coat each haze particle with butane. This is a significant amount of butane on each particle, and should form an optically thick cloud of butane in Titan's atmosphere.

However, if the butane requires a saturation ratio of $S = 1.30$ to nucleate onto the haze, as measured in this study, nucleation will (1) be occurring at a slightly lower altitude and temperature, (2) be selective and occur onto fewer haze particles, and (3) coat those particles with more butane. If nucleation occurs onto only 1 out of 10 haze particles, those particles will reach a radius of $0.23 \text{ }\mu\text{m}$ of butane. For comparison, cirrus clouds on Earth nucleate on only 1 in 10^4 background particles at a saturation ratio of $S = 1.5$. If butane selectively nucleated on 1 in 10^4 tholin particles, these particles would be coated with butane up to a radius of $1.28 \text{ }\mu\text{m}$ of butane. It can thus be seen that requiring a supersaturated condition for butane nucleation, as measured in this study, can increase the amount of butane condensed onto certain particles, while the other particles will remain bare. In contrast, a relatively low critical saturation ratio near unity will provide a homogeneous population of particles all coated with a moderate amount of butane. Therefore, the relatively high critical saturation ratio of $S_{\text{crit}} = 1.30$ measured in this study will create two distinct populations of particles lower in the atmosphere near the tropopause, where the more abundant gases methane and/or ethane will condense to form clouds. One population of these particles will be smaller in number, larger in size (several micrometers in radius), with a higher fall velocity, and coated with butane, while the other will be larger in number, smaller in size (submicrometers in radius), with a lower fall velocity, and will have bare haze material exposed. It is unclear how these distinct populations of particles will affect Titan's cloud formation, but they will probably have different effects.

It is important to note that the film used in this experiment has a much larger surface area than a single haze particle in Titan's atmosphere. The particles used in this study are agglomerates of thousands of particles with a very high surface area. The particles in Titan's atmosphere are agglomerates of ~ 30 particles which each have a radius of $\sim 0.05 \text{ }\mu\text{m}$.²⁷ Therefore, each agglomerate will have a surface area of $\sim 1 \times 10^{-8} \text{ cm}^2$. The particles in Titan's atmosphere would then have a surface area that is $\sim 2 \times 10^{-12}$ smaller than the film used in this study (assuming a surface area of 5000 cm^2). However, if we reduce the nucleation rate used in this study from $J = 1 \text{ cm}^{-2} \text{ s}^{-1}$ to $J = 2 \times 10^{-12} \text{ cm}^{-2} \text{ s}^{-1}$, the calculated value for the contact parameter, m , changes by only 0.7%. This is on the order of the experimental error. Therefore, the assumption of a nucleation rate of $J = 1 \text{ cm}^{-2} \text{ s}^{-1}$ does not significantly impact our results.

Given the smaller surface area by a factor of $\sim 10^{12}$ in Titan's atmosphere, nucleation is predicted to occur at a slightly higher

saturation ratio and thus lower temperature rather than on a longer time scale. If we assume a nucleation rate of $J = 10^{12} \text{ cm}^{-2} \text{ s}^{-1}$ instead of $J = 1 \text{ cm}^{-2} \text{ s}^{-1}$ in order to account for the smaller surface area in Titan's atmosphere, this would require an increase in S_{crit} by a factor of only 1.09, and thus nucleation would occur on the same time scale as our laboratory study but at a slightly lower temperature or higher critical saturation ratio. We find that a temperature less than one degree colder will sufficiently raise the critical saturation ratio to account for the lower surface area. The microphysical models reported by Barth and Toon^{8,37} discuss the nucleation time scales in more detail.

In addition, requiring a relatively high critical saturation ratio will affect the optical depth of the butane clouds. If nucleation occurs onto each particle at $S_{\text{crit}} = 1.0$, a butane cloud with particles of $0.13 \text{ }\mu\text{m}$ radius would form, with butane on each haze particle. The optical depth, τ , of the butane clouds can be estimated from $\tau = QN\pi r^2 L$, where Q is the extinction efficiency, N is the number of cloud particles per cubic centimeter, r is the particle radius, and L is the path length of the cloud. Assuming an extinction efficiency of $Q = 2$ in the visible wavelengths, and that the butane cloud extends to the surface (giving a path length of $L = 68 \text{ km}$), the butane cloud will have an optical depth of $\tau = 1.08$ if nucleation occurs onto each haze particle ($N = 150 \text{ cm}^{-3}$). This cloud should have a high enough optical depth to be visible.

However, if nucleation occurs onto 1 out of 10^4 particles, the particle size would be very large ($r = 1.28 \text{ }\mu\text{m}$), but nucleation would be occurring onto only $0.015 \text{ particles cm}^{-3}$. The optical depth of this cloud would be $\tau = 0.0105$, reducing the optical depth by a factor of ~ 100 . It is possible that butane clouds are removed at the tropopause by methane nucleation and subsequent sedimentation. In this case, an estimate for the cloud path length is $68 - 40 = 28 \text{ km}$. For nucleation onto every haze particle $\tau = 0.45$ and for nucleation onto 1 in 10^4 haze particles, $\tau = 0.0043$. In addition, the larger particles would quickly fall out of the atmosphere, reducing the lifetime of the cloud. Therefore, requiring a high critical saturation ratio, as measured in this study, reduces the likelihood of seeing any visible butane clouds in Titan's atmosphere.

Acknowledgment. This work was supported by the NASA Astrobiology Institute. D.B.C. was supported by a fellowship through the NASA GSRP program and NASA Ames Research Center.

V. Appendix: Application of Nucleation Theory to Butane Nucleation on Tholin Particles

The experiments described here were performed on particles much larger than those predicted to exist in Titan's atmosphere. To connect our study with smaller particles, we use heterogeneous nucleation theory.

The contact parameter for each experiment can be derived from nucleation theory and the critical saturation ratio for that experiment as follows.

The heterogeneous nucleation rate, J ($\text{cm}^{-2} \text{ s}^{-1}$), for nucleation onto a flat substrate is given by³⁸

$$J = K \exp(-\Delta G_{\text{het}}/kT) \quad (8)$$

where the free energy for heterogeneous nucleation, ΔG_{het} , is given by

$$\Delta G_{\text{het}} = [(4/3)\pi r_c^2 \sigma] f \quad (9)$$

The critical radius, r_c (cm), is related to the saturation ratio, S_{crit} (measured in our experiments), through

$$r_c = (2\sigma M_w)/(RT\rho \ln S_{\text{crit}}) \quad (10)$$

where σ (erg cm⁻²) is the interfacial energy between solid and vapor butane, ρ is the density (g cm⁻³) of the condensate, and M_w is the molecular weight (g mol⁻¹) of the condensate. The contact parameter, m , can then be extracted from the f term:

$$f = [(2 + m)(1 - m)^2]/4 \quad (11)$$

A contact parameter of $m = 1$ implies a perfect match between the condensate and substrate, such that nucleation of the condensate onto the substrate will readily occur. In contrast, $m = -1$ implies a perfect mismatch between the condensate and the substrate, such that nucleation will occur no more readily with the substrate present than without it, or as readily as homogeneous nucleation, which generally requires very high supersaturation. The pre-exponential factor, K (cm⁻² s⁻¹), in eq 8 was calculated from surface diffusion to be 10²⁵ cm⁻² s⁻¹ at the general temperature and pressure of our experiments³⁹ (1 mTorr and 125 K), but m is not sensitive to this value, as demonstrated below. If we assume $J = 1$ germ cm⁻² s⁻¹ (a *germ* is defined as the critical agglomeration of condensate molecules which will spontaneously grow upon addition of a monomer to produce a macroscopic phase change³⁸) and $K = 10^{25}$ cm⁻² s⁻¹, we can solve the above equation for m , given an experimental value for S_{crit} and T . The average contact parameter was calculated for each film experiment, assuming a flat surface, and the averages for each substrate are included in Table 2.

There are several sources of error in our determination of m . First, as stated above, there are experimental uncertainties in our determination of S_{crit} . In the worst case, varying S_{crit} by $\pm 15\%$ results in a variation in m of $\sim 2\%$. There is also uncertainty in the values of J and K . However, varying J or K by a factor of 1000 results in a change in m of $< 0.3\%$.

By far the most sensitive parameter in the determination of m is uncertainty in σ , the interfacial energy. For our calculations, we determined σ using two different methods. The first method is to use Antonoff's rule,³⁸

$$\sigma_{\text{sv}} = \sigma_{\text{sl}} + \sigma_{\text{lv}} \quad (12)$$

where σ is the interfacial energy between the different phases, denoted by s (solid), l (liquid), and v (vapor). A value for σ_{lv} was calculated to be 32.72 erg cm⁻² at 125 K,⁴⁰ while σ_{sl} was calculated from⁴¹

$$\sigma_{\text{sl}} = (0.32\Delta H_{\text{fus}})/(D^2 N_A)^{1/3} \quad (13)$$

where ΔH_{fus} (erg mol⁻¹) is the heat of fusion, D (cm³ mol⁻¹) is the molar volume, and N_A (molecules mol⁻¹) is Avogadro's number. The value for the heat of fusion used in the calculation (4.65×10^{10} erg cm⁻²) is the value at the melting point of butane (134 K). Once the value for σ_{sl} was calculated in this manner, it was added to σ_{lv} to find a total of $\sigma_{\text{sv}} = 42.29$ erg cm⁻².

The second method of calculating σ_{sv} used the formula of Guez et al.⁴²

$$\sigma_{\text{sv}} = (\Delta H_{\text{sub}}/\Delta H_{\text{vap}})^2 \sigma_{\text{lv}} \quad (14)$$

where ΔH_{sub} is the heat of sublimation (calculated from $\Delta H_{\text{vap}} + \Delta H_{\text{fus}}$). The heats of vaporization and fusion used were for two temperatures, T_b , the butane boiling point (273 K), and room

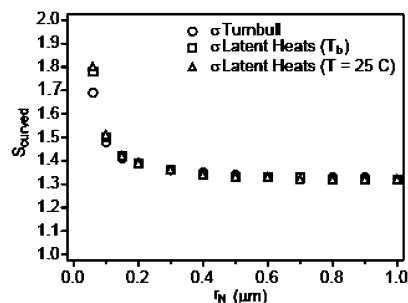


Figure 9. Critical saturation ratio for butane nucleation on tholin particles calculated from nucleation theory as a function of particle radius, r_N . Nucleation is more difficult when the substrate particles are less than $\sim 0.1 \mu\text{m}$. The surface tension term in the calculation has been determined from three different methods (see Appendix), resulting in different values, particularly at small radius.

temperature (298 K); hence, two values for σ_{sv} were calculated using this method. At T_b , σ_{sv} was calculated to be 47.69 erg cm⁻², while a value of 49.80 erg cm⁻² was calculated at room temperature. Both values of σ_{sv} calculated using eq 14 have the same temperature error as the value calculated using eq 12, in that the heats of vaporization and fusion are not known at the temperatures of our experiments (~ 125 K).

A small error in the value for σ_{sv} can lead to a large error in the value of m calculated using nucleation theory. Between the smallest value for σ_{sv} (method 1) and the largest (method 2, 298 K), the value calculated for m varies by $\sim 0.7\%$, and it is possible that a smaller value for σ_{sv} exists at our experimental temperatures. A laboratory measurement of σ_{sv} for butane is needed in order to improve the uncertainty for the m calculated from a measured S_{crit} and T .

While our tholin particles are quite large, such particles in Titan's atmosphere may be smaller, with $r = 0.1\text{--}0.2 \mu\text{m}$,³⁵ or may consist of aggregates of small curved particles;²⁷ thus, we must consider heterogeneous nucleation on curved particles in addition to nucleation on films. For a curved nucleus, the heterogeneous nucleation rate is given by³⁸

$$J = 4\pi r_N^2 K \exp(-\Delta G_{\text{het}}/kT) \quad (15)$$

where r_N is the radius of the curved substrate and the free energy for heterogeneous nucleation is given by

$$\Delta G_{\text{het}} = [(4/3)\pi r_c^2 \sigma] f_{\text{curved}} \quad (16)$$

The value for f_{curved} is calculated from Pruppacher and Klett³⁸ as

$$2f_{\text{curved}} = 1 + [(1 - mx)/\phi]^3 + x^3 \{2 - 3[(x - m)/\phi] + [(x - m)/\phi]^3\} + 3mx^2 \{[(x - m)/\phi] - 1\} \quad (17)$$

where

$$\phi = (1 - 2mx + x^2)^{1/2} \quad (18)$$

and

$$x = r_N/r_c \quad (19)$$

and all other parameters are the same as defined above.

Using this set of equations, we can relate the value for S_{crit} that would occur on a curved substrate of given radius, r_N , given the S_{crit} measured on a flat surface. An example plot is shown in Figure 9. In this example, if we measure $S_{\text{crit}} = 1.14$ (e.g., acetonitrile) on a flat surface, and calculate S_{crit} for curved

particles, it can be seen that if the curved particles were relatively small ($<0.15 \mu\text{m}$), it would raise our measured S_{crit} significantly. However, for the tholin particles used in the present study, the radius is much larger ($0.5 \mu\text{m}$), so the curvature effect should be minimal. Thus, we can directly compare our values between the tholin particles and the organic films, such that butane nucleation onto acetonitrile has the lowest S_{crit} , while tholin particles (of this size) and hexane act as similar surfaces for nucleation, each providing a higher S_{crit} than acetonitrile. For tholin particles suggested for Titan with a radius of $0.1 \mu\text{m}$,²⁷ nucleation of butane would require a higher S_{crit} of 1.5.

References and Notes

- (1) Lindal, G. F.; Wood, G. E.; Hotz, H. B.; Sweetnam, D. N.; Eshleman, V. R.; Tyler, G. L. *Icarus* **1983**, *53*, 348.
- (2) Hanel, R.; Conrath, B.; Flasar, F. M.; Kunde, V.; Maguire, W.; Pearl, J.; Pirraglia, J.; Samuelson, R.; Herath, L.; Allison, M.; Cruikshank, D.; Gautier, D.; Gierasch, P.; Horn, L.; Koppany, R. *Science* **1981**, *212*, 192.
- (3) Sagan, C.; Thompson, W. R. *Icarus* **1984**, *59*, 133.
- (4) Khare, B. N.; Sagan, C.; Arakawa, E. T.; Suits, F.; Callcott, T. A.; Williams, M. W. *Icarus* **1984**, *60*, 127.
- (5) Miller, S. L. *Science* **1953**, *117*, 528.
- (6) Miller, S. L. *J. Am. Chem. Soc.* **1955**, *77*, 2351.
- (7) Sagan, C.; Khare, B. N. *Nature* **1979**, *277*, 102.
- (8) Barth, E.; Toon, O. *Icarus* **2003**, *162*, 94.
- (9) Lunine, J. I.; Stevenson, D. J.; Yung, Y. L. *Science* **1983**, *222*, 1229.
- (10) Campbell, D.; Black, G.; Carter, L.; Ostro, S. *Science* **2003**, *302*, 431.
- (11) Courtin, R.; Gautier, D.; McKay, C. P. *Icarus* **1995**, *114*, 144.
- (12) McKay, C. P.; Martin, S. C.; Griffith, C. A.; Keller, R. M. *Icarus* **1997**, *129*, 498.
- (13) Samuelson, R. E.; Nath, N. R.; Borysow, A. *Planet. Space Sci.* **1997**, *45*, 959.
- (14) McKay, C. P. *Planet. Space Sci.* **1996**, *44*, 741.
- (15) Griffith, C. A.; Owen, T.; Miller, G. A.; Geballe, T. *Nature* **1998**, *395*, 575.
- (16) Griffith, C. A.; Hall, J. L.; Geballe, T. R. *Science* **2000**, *290*, 509.
- (17) Brown, M. E.; Bouchez, A. H.; Griffith, C. A. *Nature* **2002**, *240*, 795.
- (18) Roe, H.; DePater, I.; Macintosh, B.; McKay, C. *Astrophys. J.* **2002**, *581*, 1399.
- (19) Moses, J. I.; Allen, M.; Yung, Y. *Icarus* **1992**, *99*, 318.
- (20) Lara, L.; Lellouch, E.; Lopez-Moreno, J.; Rodrigo, R. *J. Geophys. Res.* **1996**, *101*, 23.
- (21) Adamkovics, M.; Boering, K. A. *J. Geophys. Res.* **2003**, *108*, 5092.
- (22) Dodonova, N. Y. *Russ. J. Phys. Chem.* **1966**, *40*, 523.
- (23) Clarke, D. W.; Joseph, J. C.; Ferris, J. P. *Icarus* **2000**, *147*, 282.
- (24) de Vanssay, E.; McDonald, G. D.; Khare, B. N. *Planet. Space Sci.* **1999**, *47*, 433.
- (25) Sanchez, R. A.; Ferris, J. P.; Orgel, L. E. *Science* **1966**, *154*, 784.
- (26) McDonald, G. D.; Thompson, W. R.; Heinrich, M.; Khare, B. N.; Sagan, C. *Icarus* **1994**, *103*, 137.
- (27) McKay, C. P.; Coustenis, A.; Samuelson, R. E.; Lemmon, M. T.; Lorenz, R. D.; Cabane, M.; Rannou, P.; Drossart, P. *Planet. Space Sci.* **2001**, *49*, 79.
- (28) Lebonnios, S.; Bakes, E.; McKay, C. *Icarus* **2002**, *159*, 505.
- (29) Sagan, C.; Khare, B. N.; Lewis, J. S. Organic matter in the Saturn system. In *Saturn*; Gehrels, T., Matthews, M. S., Eds.; University of Arizona Press: Tucson, AZ, 1984; p 788.
- (30) Tran, B. N.; Ferris, J. P.; Chera, J. J. *Icarus* **2003**, *162*, 114.
- (31) Coll, P.; Coscia, D.; Gazeau, M. C.; de Vanssay, E.; Guillemin, J. C.; Raulin, F. *Adv. Space Res.* **1995**, *16*, 93.
- (32) Coll, P.; Coscia, D.; Smith, N.; Gazeau, M. C.; Ramirez, S. I.; Cernogora, G.; Israel, G.; Raulin, F. *Planet. Space Sci.* **1999**, *47*, 1331.
- (33) Silverstein, R. M.; Bassler, G. C.; Morrill, T. C. *Spectrometric Identification of Organic Compounds*, 5th ed.; John Wiley and Sons: New York, 1991.
- (34) Tolbert, M. A.; Middlebrook, A. M. *J. Geophys. Res.* **1990**, *95*, 22423.
- (35) Toon, O.; McKay, C.; Griffith, C.; Turco, R. *Icarus* **1992**, *95*, 24.
- (36) Toon, O. B.; McKay, C. P.; Courtin, R.; Ackerman, T. P. *Icarus* **1988**, *75*, 255.
- (37) Barth, E.; Toon, O. *Geophys. Res. Lett.* **2004**, *31*, L17S01.
- (38) Pruppacher, H. R.; Klett, J. D. *Microphysics of clouds and precipitation*; Kluwer Academic Publishing: Dordrecht, The Netherlands, 1997.
- (39) Fletcher, N. H. *The Physics of Rainclouds*, 1st ed.; The Syndics of the Cambridge University Press: Cambridge, 1962.
- (40) Jasper, J. J. *J. Phys. Chem. Ref. Data* **1972**, *1*, 841.
- (41) Turnbull, D. *J. Appl. Phys.* **1950**, *21*, 1022.
- (42) Guez, L.; Bruston, P.; Raulin, F.; Regnaut, C. *Planet. Space Sci.* **1997**, *45*, 611.